CFD ANALYSIS OF ENGINE AIR INTAKE FOR A PUSHER TYPE LIGHT TRANSPORT AIRCRAFT

Vinay C A 1 [1*], Kumar G N 2 [2], Bhaskar Chakravarthy 3 [1] Venkat Iyengar 4 [1], HNV Dutt 5 [1]

[1]National Aerospace Laboratories, Bangalore, Karnataka, India, 560017
[2]Department of Mechanical Engineering, NITK-Surathkal, Mangalore, Karnataka. India, 575 025

ABSTRACT

In the process of design, development and certification of a turbo-prop Light Transport Aircraft (LTA), an important aspect is to establish the installed performance of the engine before carrying out actual flight tests. In this context, it is relevant to study and analyse behaviour of the engine air intake performance before commencing actual flight tests. CFD analysis of flow in and around the nacelle and engine air intake duct was carried out using two RANS based models, S-A and SST k-omega using the commercial software ANSYS Fluent. Special emphasis was laid on developing a good quality mesh for the computational domain with a finer boundary layer mesh along the wall and by maintaining a higher density mesh at critical areas. Ram air recovery and mass flow rate of main air intake duct has been established from the results obtained. The results obtained from the CFD study have shown that the inlet system pressure loss and ram air recovery are within limits prescribed by the engine original equipment manufacturer. From the overall analysis, total pressure total pressure recovery at the plenum was found satisfactory for all flight cases, covering variation in the Mach number, altitude and nacelle AOA. Qualitative results obtained from CFD show that the behaviour of the engine intake is consistent across flight conditions.

Keywords: Nacelle, engine, pressure loss, ram recovery, air intake, bypass duct;

1. INTRODUCTION

Turboprop engines are widely used in commuter category airplanes. The air intake for a pusher configured turbo-prop engine has been designed following the guidelines given in the installation handbook, provided by the engine original equipment manufacturer (OEM). The objectives for the design are efficient ram pressure recovery at the engine air inlet leading to maximum possible total pressure at the air inlet screen over a wide range of normal flight conditions, this is required to obtain maximum power levels and low specific fuel consumption. Nacelle and engine configuration is shown in fig.1.

The general goals were to analyze the flow field around the engine nacelle and in whole intake section using the CFD method and to estimate intake pressure loss and ram recovery for various flight cases during non icing condition. The CFD package ANSYS Fluent 13.0 was used to model this problem. The finite volume method was implemented for numerical solution of the Navier-Stokes equation with choice of different models for turbulence [2].

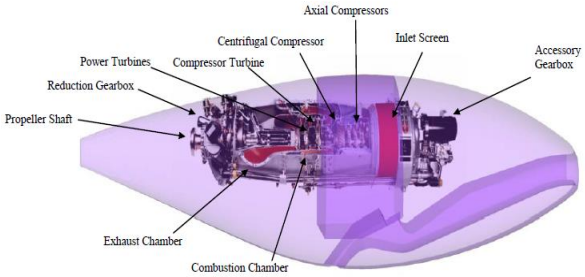

Fig.1: Air Intake Duct, Nacelle and Engine Integration

Computation run was done at CSIR-NAL HPC facility for solution and post processing. HP Z800 four processor workstation was used for pre-processing.

2. DATA PREPARATION

2.1. Geometric Simplification

One consideration when dealing with such a complex problem is to be as realistic as possible. On the other hand there are constraints, when modeling geometric details e.g. minimizing solver time while reducing the meshing effort etc. Therefore it was decided to neglect

* vinay.ca@nal.res.in

minor and inconsequential structural details. Also, the propeller and spinner assembly was not considered and the propeller hub (downstream) portion was replaced by a smooth contour near the aft end of the nacelle see Fig 2.

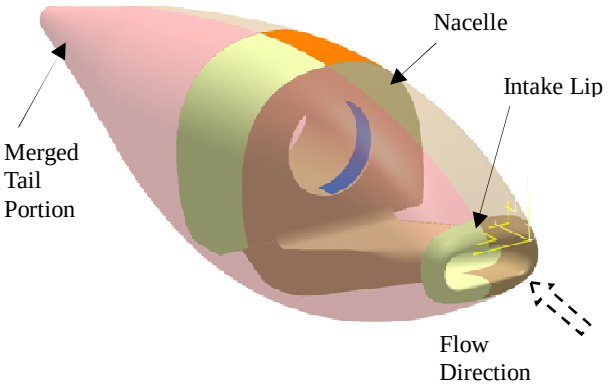

Fig. 2. External Part of Nacelle Geometry

2.2. Geometry

The geometry of the nacelle and air intake was created from 2D lofting. The CATIA V5 R17 CAD system was used for digitizing the geometric data. Points, curves and surfaces were used to describe the geometric layout. The geometry involves an external part and an internal part. The external parts consist of the nacelle see Fig. 2. The internal part consists of the nacelle, featuring the air intake duct, bypass duct and inertial particle separator door and the engine protection screen (Fig.3). For importing CAD data into the ANSYS Fluent pre-processor an IGES file was created.

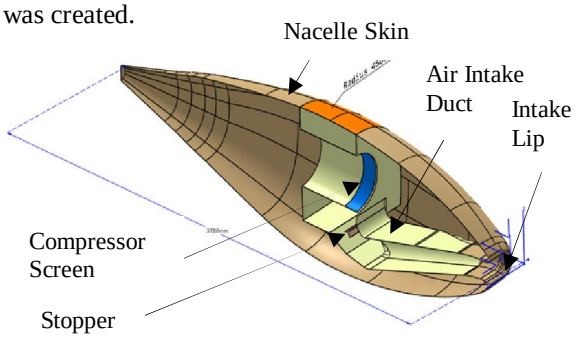

Fig.3. Internal Part of Nacelle Geometry

2.3. Computational Domain

For pre-processing, ANSYS ICEM CFD was used to prepare data for the solver. The IGES file was imported into pre-processor, where the geometry was reconstructed and a solid for whole computational domain was created. The domain consists of a semi-cylindrical front part and rear part. As the creation of the solid was successfully performed, surface seeds, the setting of prismatic elements and volume mesh refinement controls were applied at expected areas of flow variation and a volume mesh was generated. Setting appropriate values of mesh controls was a difficult task due to the geometric complexity of the model. A number of elements in the unstructured mesh varied up to 11.4 millions. The surface mesh is shown at Fig. 4.

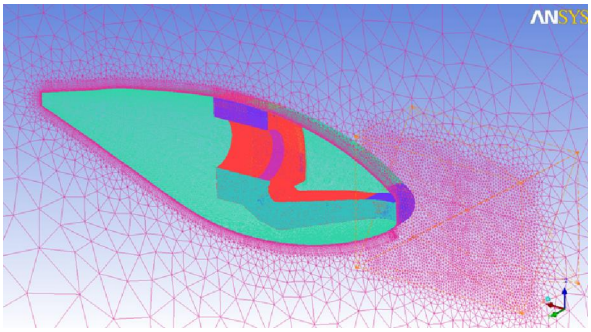

Fig. 4 Surface Mesh at Nacelle and Symmetry Plane

2.4. Boundary Conditions

The task was setup with a plane of symmetry in order to decrease solution time. The boundary conditions (BC) were chosen as follows. For free stream input into a domain, a velocity-inlet (ñInletò) was used, an ñOuter wallò was defined as a wall with no slip, an ñOutletò was defined as a pressure-outlet from the domain. For the ñNacelleò it is used as a wall, at the ñCompressor inputò pressure-outlet was defined (from the domainôs point of view it is in fact output of the flow). See Fig. 5 and 6.

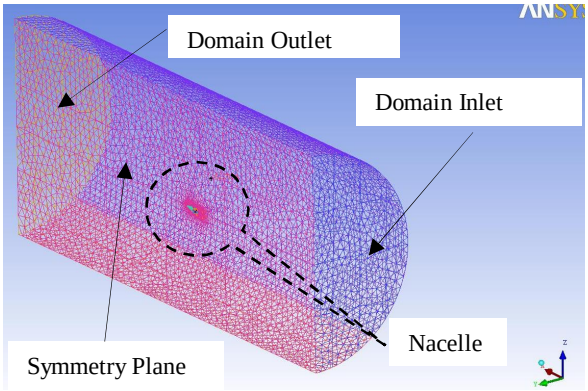

Fig. 5 Global BC

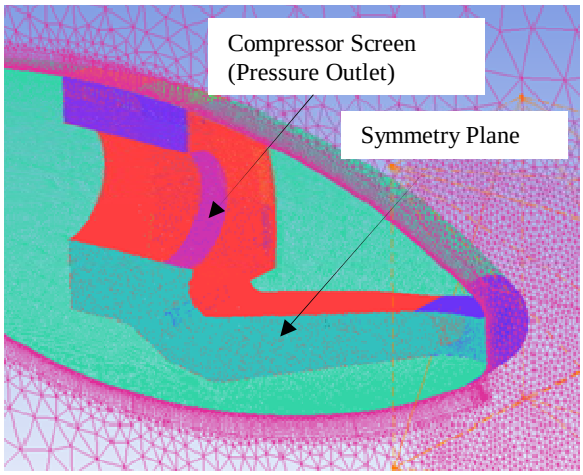

Fig. 6 BC at Nacelle

2.5. Monitoring Surfaces

For the computed case, comparison sets of monitor surfaces were defined to determine the flow characteristics in these sections (see Fig. 7).

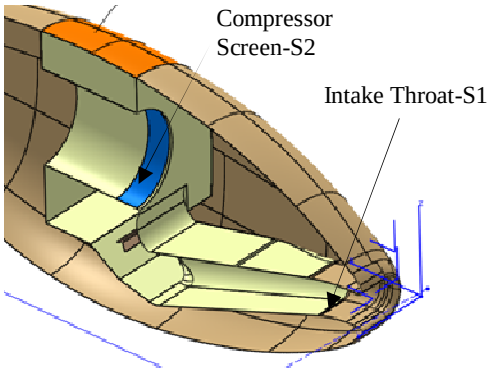

Fig. 7 Monitoring Surfaces in air intake duct and bypass duct

2.6. Flow Parameters and Solver Setting

All computations were done with the parameters mentioned in Table 1 and 2. The fluid was modeled as incompressible or compressible gas for low and high flight speeds respectively. The influence of the propeller was not modeled and the propeller slipstream was neglected (this allows a single symmetry plane to be used). A turbulence intensity value of five percent behind the nacelle was assumed. All solver runs were realized as parallel on the computers. The tasks were setup for a steady state solution.

Table 1: Flight Conditions and inputs for analysis

Case No.	Altitude, m (ft)	Free Stream Total Pressure, Pa	Free Stream Static Pressure, Pa
1	1372 (4500)	88578	85908.6
2	3810 (12500)	66222	63190.5
3	7620 (25000)	43743	37576.4
4	7620 (25000)	41983	37576.4
5	4572 (15000)	61661	57157.5
6	914 (3000)	91709	91700

Table 2: Flight Conditions and inputs for analysis continued

Case No.	Outside Air Temperature °C, (K)	Speed m/s (M)	Engine Mass Flow Rate, Kg/s (lb/s)	Nacelle Angle of Attack, deg
1	6.1 (279.25)	71.4 (0.21)	4.036 (8.90)	6.60
2	9.75 (263.4)	88.4 (0.26)	3.43 (7.61)	5.45
3	-34.5 (238.65)	159.9 (0.47)	2.56 (5.65)	0.90
4	-34.5 (238.65)	136.2 (0.4)	2.5 (5.50)	2.67
5	-14.5 (258.45)	112.3 (0.33)	3.22 (7.08)	2.56
6	34 (307.15)	6.8 (0.02)	5.0 (11.0)	0

.

3. COMPUTED CASES

3.1. Computation Process

The ANSYS FLUENT 13.0 Solver was used for all computations. The solution time per case varied up to a few days. The computation process had always the same scheme. Firstly, in several steps, the mass flow ratio through the engine was ñtunedò by setting the value of mass flow target at BC ñCompressor inputò (the engine mass flow value was given for all the flight conditions). The allowable differences between the two known and computed values were set as ±3%. After the computation reached a value for all maximal residuals under $1x10^{-4}$ the solution was declared as converged.

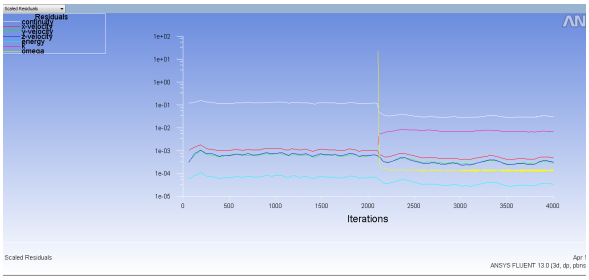

Fig. 8: Typical history of convergence, for original air intake turbulence model k-Omega

3.2. Solutions

The main goal in this project was to assess the intake performance intake pressure loss and ram recovery during non icing condition for different flight cases. In all cases the k-omega SST turbulence model was used, [1] [3] except for the cases number 1, 2 and 6 where an S-A model was used and with an automatic wall treatment.

3.3. Flow Visualization

The main flow characteristics were monitored at surfaces S1ï S2, and the total pressure losses and ram recovery in the internal sections were determined see Fig 9.0 to 23.0 and Table 3, 4 and 5.

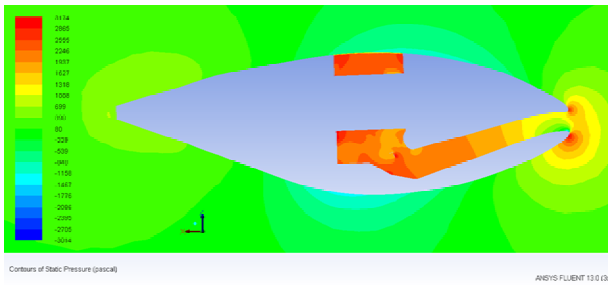

Fig.9 Case 1: Flow Fields- Boundary Surfaces Static Pressure Maps, S-A turbulence model

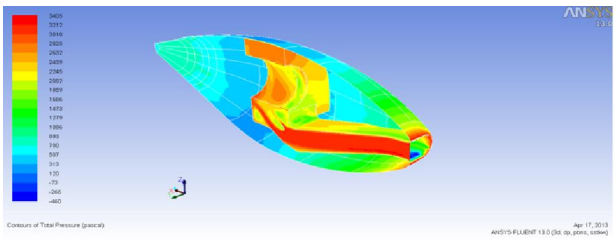

Fig.10 Case 1: Flow Fields- Boundary Surfaces Total Pressure Maps, S-A turbulence model

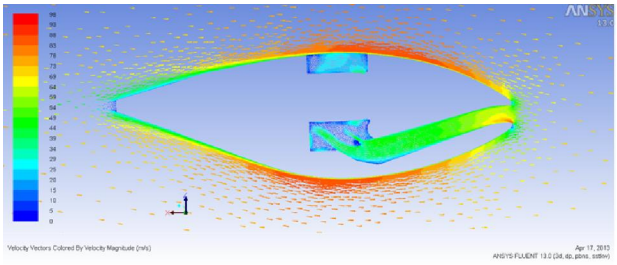

Fig.11 Case 1: Flow Fields- Velocity Vector, S-A turbulence model

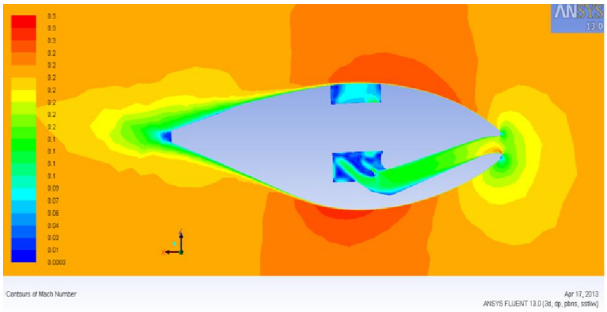

Fig.12 Case 1: Flow Fields- Symmetry Plane Mach number Maps, S-A turbulence model

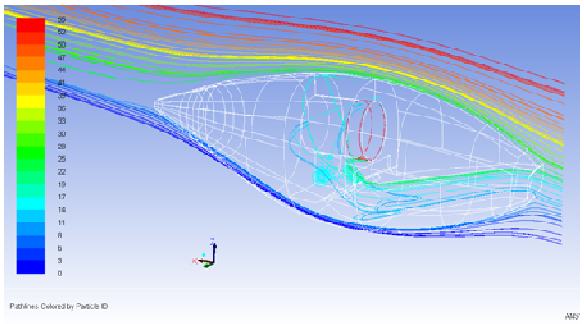

Fig.13 Case 1: Flow Fields- Pathlines, S-A turbulence model

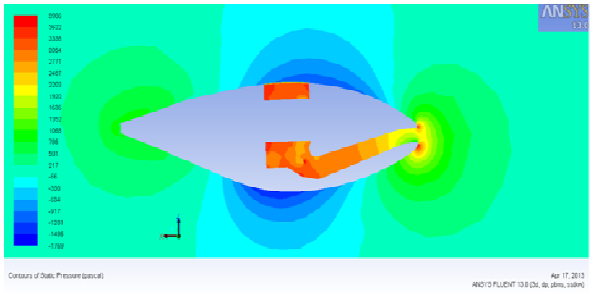

Fig.14 Case 2: Flow Fields- Boundary Surfaces Static Pressure Maps, S-A turbulence model

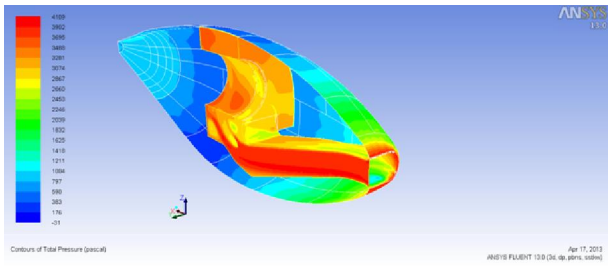

Fig.15 Case 2: Flow Fields- Boundary Surfaces Total Pressure Maps, S-A turbulence model

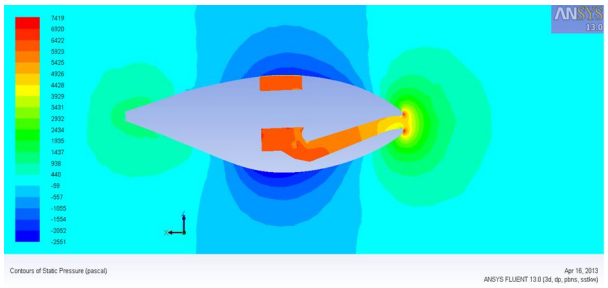

Fig.16 Case 3: Flow Fields- Boundary Surfaces Static Pressure Maps, S-A turbulence model

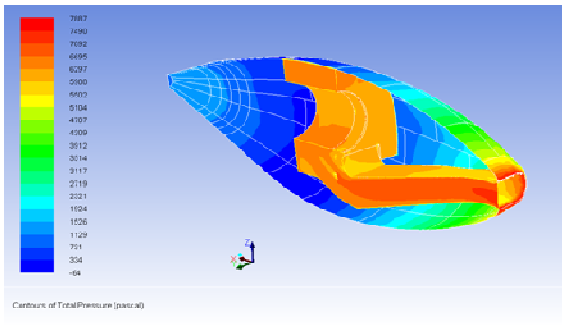

Fig.17 Case 3: Flow Fields- Boundary Surfaces Total Pressure Maps, S-A turbulence model

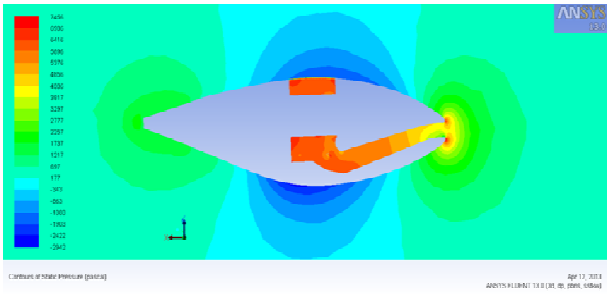

Fig.18 Case 4: Flow Fields- Boundary Surfaces Static Pressure Maps, S-A turbulence model

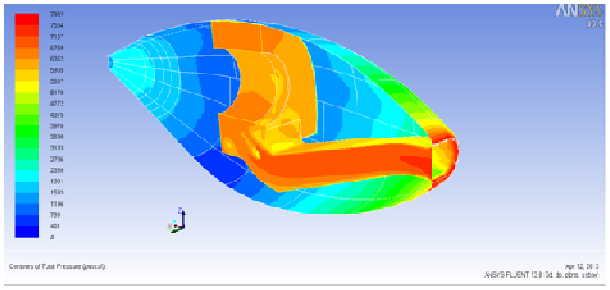

Fig.19 Case 4: Flow Fields- Boundary Surfaces Total Pressure Maps, S-A turbulence model

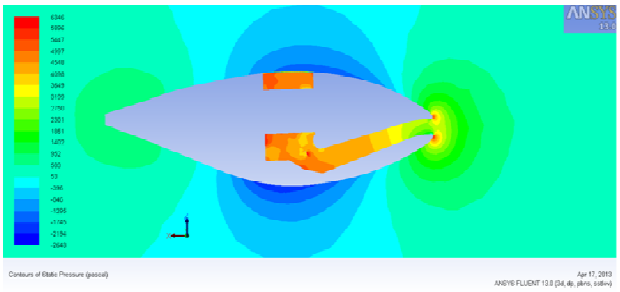

Fig.20 Case 5: Flow Fields- Boundary Surfaces Static Pressure Maps, S-A turbulence model

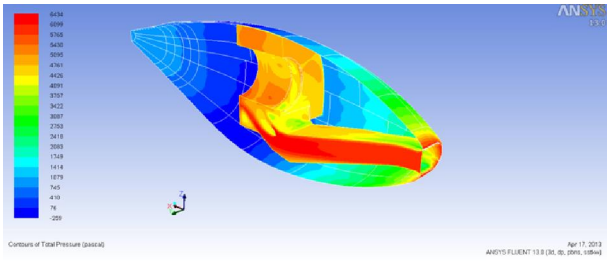

Fig.21 Case 5: Flow Fields- Boundary Surfaces Total Pressure Maps, S-A turbulence model

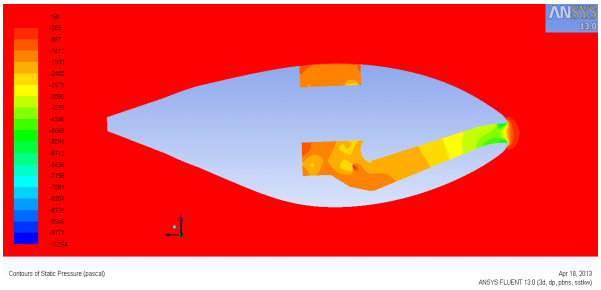

Fig.22 Case 6: Flow Fields- Boundary Surfaces Static Pressure Maps, S-A turbulence model

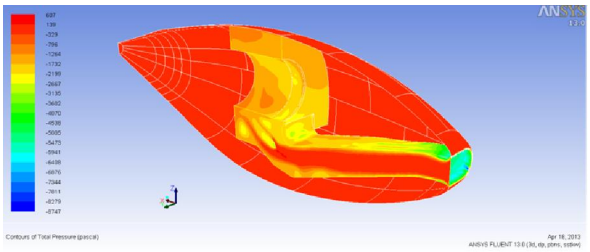

Fig.23 Case 6: Flow Fields- Boundary Surfaces Total Pressure Maps, S-A turbulence model

Table 3: Computational Results

Case No.	Altitude m	Compressor Screen		
		Dynamic Pressure, Pa	Static Pr, Pa	Total Pr, Pa
1	1371.6	565	1578	2160
2	3810	514	2484	3012
3	7620	457	5603	6060
4	7620	593	5424	6017
5	4572	910	4037	4967
6	914.4	920.8	-2836	8.6

Table 4: Computational Results Continued

Case No.	Altitude m	Inlet (Throat)		
		Dynamic Pressure, Pa	Static Pr, Pa	Total Pr, Pa
1	1371.6	2783	10.5	2794
2	3810	3428	19	3446
3	7620	6278	190	6468
4	7620	6023	471	6494
5	4572	5231	5.2	5397
6	914.4	8.2	0.5	-1888

3.4. Sample Calculation

Case No. 1

A. Inlet Pressure Loss:

Inlet pressure loss is defined as the percentage total pressure drop that occurs in the aircraft inlet system. It is defined as:

$$\text{Inlet Pressure Loss} = \frac{\Delta P}{P} = \frac{P_0 - P_1}{P_0} \qquad (1)$$

Where

P_0= Free Stream Total Inlet Pressure

P_1= Engine Inlet screen total pressure

$$\text{Inlet Pressure Loss} = \frac{\Delta P}{P} = \frac{2794 - 2160}{88578} X100 = 0.72\%$$

B. Ram Recovery:

Ram recovery is a measure of the ability of the aircraft inlet system to convert free stream dynamic pressure into static pressure at the engine inlet screen. It is defined as:

$$\text{Ram recovery} = \frac{P_1 - P_{amb}}{P_0 - P_{amb}} \qquad (2)$$

Where

P_1= Engine Inlet Screen Total Pressure, psi

P_0= Free Stream Total Inlet Pressure, psi

P_{amb}= Free Stream Static Pressure, psi

$$\text{Ram recovery} = \frac{2160}{2794} X100 = 77.3\%$$

Similarly, for the remaining cases (case 2 to 6) results have been tabulated in Table 5.

Table 5: Analysis of Results

Case No.	Engine Mass Flow, Kg/s	$(\varphi P/P)_{IN}$ De-Icing off, % (Non Icing)	RAM RECOVERY, %
1	4.05	0.72	77.3
2	3.5	0.66	87.4
3	2.5	0.93	93.7
4	2.4	1.2	92.7
5	3.2	1	92.0
6	5	2.06	Not Applicable

4. RESULTS AND CONCLUSIONS

This paper presents CFD for the engine air intake of LTA using Ansys Fluent. Simulations were carried out for various flight conditions as per Table 1 for bypass duct closed conditions (non-Icing) to determine the engine intake pressure loss and mass flow characteristics of intake duct.

From static pressure plots see Fig 9, 14, 16, 18, 20 and 22 it is observed that the low pressure region in the lower portion of nacelle. From total pressure plot see Fig 10, 15,17,19,21 and 23 it is clearly observed that total pressure is adequately recovered between the intake lip and engine intake (plenum) while meeting the engine mass flow requirements (MFR). Similar qualitative behavior can be seen in all the flight cases considered (case no.1 to 5). Quantitative results are tabulated in Table 5. From the overall analysis, total pressure recovery was found very good in all flight cases irrespective of variations in flight conditions such as variation in Mach number, altitude and AOA. Inlet pressure losses obtained by CFD computations are in good agreement in comparison with OEM supplied typical values.

5. ACKNOWLEDGEMENTS

The authors wish to thank all partners and associated partners for their contribution to the program and for their permission to publish this paper.

6. REFERENCES

[1] Guilherme L. Oliveira, Luis C. C. Santos, André L. Martins, Gilberto G. Becker, Marcus V. F. Reis, Nicolas Spogis and Rodrigo F. A. F. Silva (2008). ñA Tool for Parametric Geometry and Grid Generation for Aircraft Configurationsò, ICAS 2008, Embraer ï Empresa Brasileira de Aeronáutica, Brazil, ESSS - Engineering Simulation and Scientific Software, Brazil

[2] Jiyuan Tu, Guan Heng Yeoh and Chaoqun Liu (2008). ñ*Computational Fluid Dynamics: A Practical Approach*ò, First Edition, Elsevier, USA.

[3] Zhidong Wang, Meihong Zhang and Junhong Wang (2006). ñA Study On Aerodynamic Design Integration of the Supercritical Wing and Rear mounted Engine Configurationò, ICAS 2006, First Aircraft Design and Research Institute, Shanghai, China.